JMEPEG (2004) 13:151-157
DOI: 10.1361/10599490418343

1059-9495/$19.00

Load Relaxation of Helical Extension Springs in Transient Thermal Environments

R.C. Dykhuizen and C.V. Robino

(Submitted 21 July 2003; in revised form 9 January 2004)

The load relaxation behavior of small Elgiloy helical extension springs has been evaluated by a combined experimental and modeling approach. Isothermal, continuous heating, and interrupted heating relaxation tests of a specific spring design were conducted. Spring constants also were measured and compared with predictions using common spring formulas. For the constant heating rate relaxation tests, it was found that the springs retained their strength to higher temperatures at higher heating rates. A model, which describes the relaxation behavior, was developed and calibrated with the isothermal load relaxation tests. The model incorporates both time-independent deformation mechanisms, such as thermal expansion and shear modulus changes, as well as time-dependent mechanisms such as primary and steady state creep. The model was shown to accurately predict the load relaxation behavior for the continuous heating tests, as well as for a complex stepwise heating thermal cycle. The model can be used to determine the relaxation behavior for any arbitrary thermal cycle. An extension of the model to other spring designs is discussed.

Keywords: heating relaxation, helical extension springs, isothermal heating

1. Introduction

Springs are used in many applications to provide a constant force at a constant displacement. For example, the force on locking pawls or ball detents is generally applied by springs loaded at a constant displacement. The exposure of spring-loaded assemblies to temperatures above the normal design operating temperature range can cause the force applied by the springs to change. In turn, these changes can be the result of a variety of factors, including thermal expansion of the spring and assembly, reduction of the (elastic or shear) modulus on increasing temperature, microstructural changes such as loss of temper or overaging, and, finally, plastic creep. When a spring is used in a safety-critical application that may be exposed to an abnormal thermal environment, it is necessary to quantify the relaxation behavior of the spring during the thermal transient.

Typical design guides for springs (e.g., Ref. 1) do not treat this type of relaxation since it is beyond the scope of normal design practice. However, constant temperature (usually RT or storage temperature) relaxation has been considered,[2] and guidance for stress relaxation testing of spring materials is available.[3] In this approach to determining relaxation rates, the material-specific relaxation behavior is determined through isothermal stress relaxation tests on wire or strip, and the results are applied to specific spring designs through the application of various spring stress-state equations and geometric corrections.[1,2] This approach generally requires making some assumptions regarding the actual stress state in the loaded spring, and it is difficult to account for residual stresses that develop in the spring material during forming operations. Conversely, direct load relaxation testing of actual springs can be conducted to determine the response of specific designs. This approach inherently provides information regarding the effects of residual stresses and the complex stress states that exist in real springs (such as in the hooks of extension springs), but it is difficult to determine how this information is best transferred to springs of different designs and/or different materials. This latter approach was taken in the current study.

The complexity is increased further in the case of non-isothermal temperature excursions. Depending on the range of temperatures involved, the relative contributions of the various force reduction mechanisms can vary with temperature. Thus, while thermal expansion and reduction in the modulus may be the primary factors controlling load at lower temperatures, creep may be the dominant factor at higher temperatures. Furthermore, depending on the time and temperature scales involved, the relative contributions of primary and steady-state creep may be different.

The goal of this work was to develop a methodology for assessing the relaxation behavior of extension springs during non-isothermal temperature transients. Toward this end, the relaxation was evaluated through experimental measurements. From these measurements, a model of the various processes was developed. The model then was shown to accurately predict the spring response for a variety of thermal transients. To illustrate the methodology, results are presented here for a specific spring design and loading conditions over a wide range of thermal transients. The extension of this approach to other spring designs will be discussed briefly in this report.

2. Experimental Procedures

The basic nominal dimensions of the spring used in this investigation are shown in Fig. 1. The springs were fabricated from Elgiloy (a registered trademark of Elgiloy Specialty Metals, Elgin IL) with a nominal composition of 40 Co-20 Cr-15

R.C. Dykhuizen and **C.V. Robino,** Sandia National Laboratories, Albuquerque, NM 87185. Contact e-mail: rcdykhu@sandia.gov.

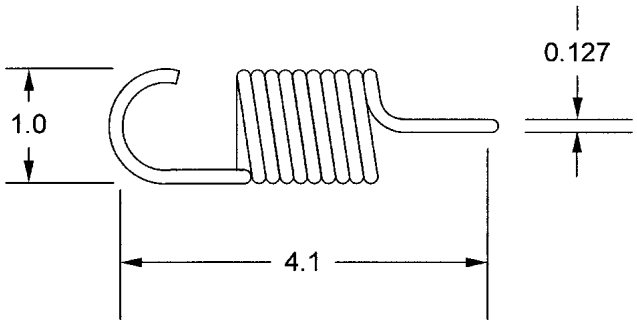

Fig. 1 Drawing of the spring used in this investigation (dimensions are in millimeters). The spring is composed of 9.25 turns.

Ni-7 Mo-2 Mn-15 Fe-0.15 C-0.05 Be by weight. The springs were wound from 0.127 mm diameter wire in the annealed plus cold drawn 46% condition and were aged 5 h at 510 °C following winding.

Extension and load relaxation tests were conducted on a servo-hydraulic load frame fitted with induction heating coils for temperature control, as shown in Fig. 2(a). A type 304 stainless steel tube (9.3 mm ID, 11.4 mm OD, and 89 mm in length) was used as a susceptor to ensure uniform heating of the spring and was located inside an alumina tube. Connection to the spring was made by means of quartz extension rods and alumel wire hooks. A calibrated 5N load cell was used for force measurements. A 0.254 mm diameter sheathed type K thermocouple was used to monitor the spring temperature, as shown in Fig. 2(b)

A series of uniaxial loading tests was used to determine the spring constant as a function of temperature. These tests were conducted following stabilization of the temperature (typically about 1 min) and were conducted at an extension rate of 0.1 mm/s. For these tests, the spring constant was taken as the slope of the initial linear portion of the load/extension curve. For isothermal stress relaxation tests, the furnace and sample were first stabilized at 150 °C, and the spring then was loaded to a force of 450 mN (1.2 mm extension). At this point, the load frame crosshead was locked in place, and the temperature then was ramped at a heating rate of 200 °C/min to the isothermal hold temperature. Load was monitored throughout the heating, hold, and cooling cycles.

Linear heating rate load relaxation tests were conducted at heating rates of 5, 10, 20, 50, and 100 °C/min. As with the isothermal relaxation tests, the temperature was first stabilized at 150 °C prior to load (450 mN) application.

3. Results

Figure 3 shows the typical load/extension curves for the spring at 300 and 600 °C. As expected, both the spring constant and the onset of plastic yielding decreased with increasing temperature.

In Fig. 4, the experimental spring constants were obtained from measurements of the spring force as a function of displacement at each of the temperatures. Also shown are estimates of the spring constant based on the spring dimensions and acoustic measurements of the shear modulus for Elgiloy (Fig. 5)[4,5] and the standard equation for extension springs,[1]

$$k = \frac{Gd^4}{8D^3N} \quad \text{(Eq 1)}$$

where G is the shear modulus (which is a function of temperature), d is the wire diameter, D is the coil diameter, and N is the number of coil turns. Several different calculations of the spring constant are shown, all of which used the acoustic measurements of the shear modulus. Due to testing constraints, not all of the individual springs that were tested could be measured prior to testing. Therefore, several different approaches were used in the calculations of spring constants. The first of these was to use the nominal spring dimensions taken directly from the design drawing. In addition, the relevant dimensions of five separate springs from the same lot were accurately measured, and the resulting spring constants (from Eq 1) are also shown. Finally, the average dimensions of the five measured springs are used to determine the spring constant.

Figure 4 has several important implications. At temperatures below 500 °C, Eq 1 yields an accurate estimate of the spring constant, provided that accurate measurements of the spring dimensions are used. Thus, it is believed that Eq 1 is reasonable for use in design. As discussed later, this agreement implies that generalization of the current relaxation model to other extension spring geometries can, in part, be accomplished through modeling equations. For Elgiloy springs at temperatures above 500 °C, the experimental spring constants deviate substantially from the estimated values. This deviation is the result of time-dependent plastic deformation (creep) of the spring during testing and is not the result of inaccuracies in Eq 1.

The load-displacement tests also indicated the elastic limit of the spring as a function of temperature. Although these are not discussed here, it is important to note that the displacement of 1.2 mm (which corresponds to a 150 °C preload of approximately 450 mN) is beyond the proportional limit for the spring at 700 °C.

Figure 6 shows the results of the fixed-displacement heating relaxation tests. For the fixed spring displacement, heating produces a reduction of the force that the spring applies. This reduction in spring force is due to several mechanisms, including changes in shear modulus with temperature, the thermal expansion of the spring and assembly (grip) materials, and stress relaxation (plastic creep). The first two of these mechanisms are reversible with temperature (assuming no significant microstructural changes) and do not produce permanent plastic deformation. The last mechanism results in permanent, irreversible plastic deformation that is not recovered on cooling. Moreover, because creep stress relaxation is a time-dependent phenomenon, the amount of this deformation is a function of the temperature history of the spring and not just the instantaneous temperature. Extension springs that are heated more rapidly can be expected to retain a given tensile force to higher temperatures than springs that are heated more slowly, and this is observed in Fig. 6. On heating, the two reversible mechanisms described above produce an initial reduction in the spring force. At temperatures above about

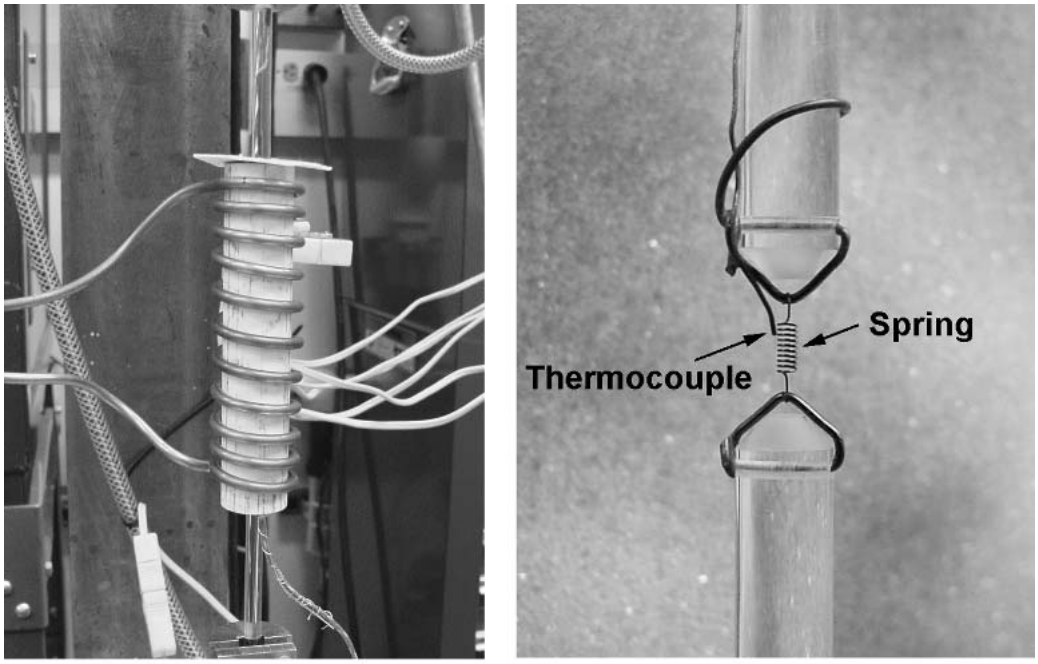

Fig. 2 Photographs of the test setup. **(a)** Induction heating coils and insulation; **(b)** sample grips and thermocouple location

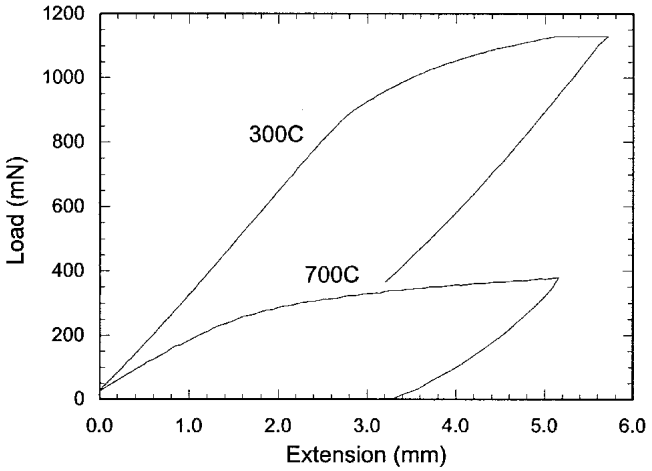

Fig. 3 Typical load/extension curves for Elgiloy spring at 300 and 600 °C

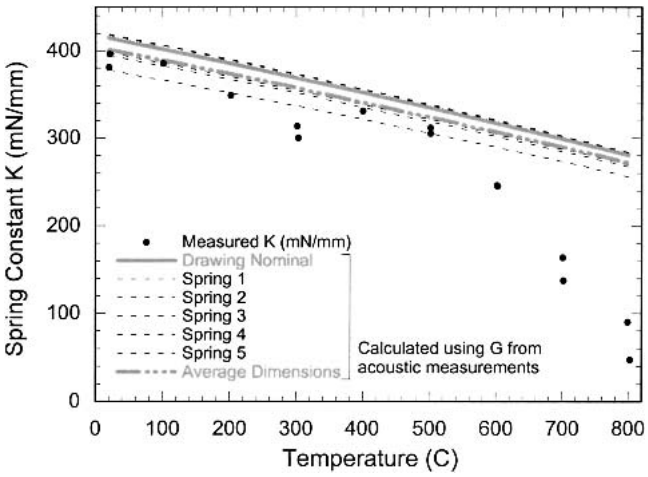

Fig. 4 Comparison of measured and calculated spring constants

450 °C, the reduction in spring force degrades more rapidly and is a function of the heating rate (i.e., the spring retains higher forces with higher temperatures at higher heating rates). During cooling, the spring elastically recovers some force, but, due to the plastic deformation that occurred at high temperature, the final force is only a fraction of the initial force.

Ultimately, the development of the capability for computing the spring force for any given set of initial conditions for any spring design at any time during an arbitrary time-temperature exposure is desired. Toward this goal, an analytical model has been developed that accounts for the various force reduction mechanisms.

3.1 Analytical Model

A model was developed to determine the spring force as a function of time and temperature. The starting point of the model is the simple spring force linear relationship:

$$F = k\{X - [X_0 + X_0(\alpha(T - T_0) + \varepsilon)]\} \quad \text{(Eq 2)}$$

where k is the spring constant, X is the spring displacement, α is the coefficient of thermal expansion, X_0 is the initial spring length, T is the temperature, T_0 is a reference temperature, and ε is the integrated creep of the spring material. In the current application, the spring displacement is maintained nominally constant, and this approach was maintained during all of the

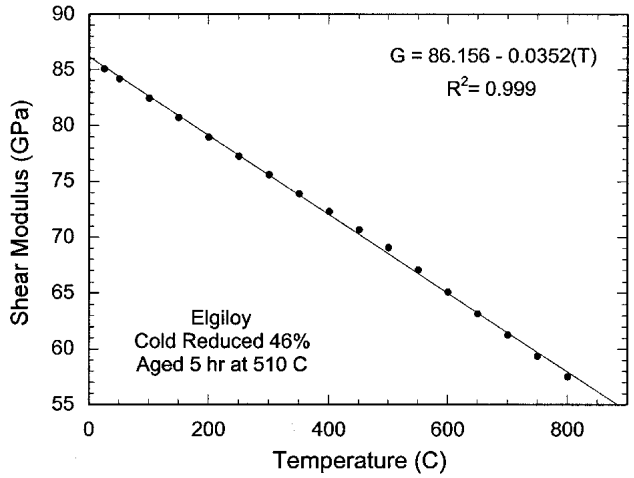

Fig. 5 Shear modulus for Elgiloy in the cold-reduced and aged condition, as determined by acoustic measurements[4]

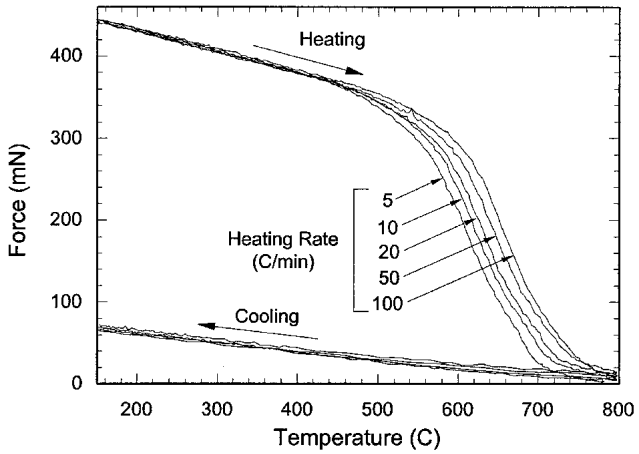

Fig. 6 Force at constant displacement as a function of temperature for a variety of heating rates between 5 and 100 °C/min. For higher heating rates, the spring force is higher at temperatures between 500 °C and 800 °C (spring preloaded to 450 mN at 150 °C).

relaxation experiments described here. However, it was determined that one must accurately account for the thermal expansion of the fixture (including the quartz extension rods and grip wires), which changes the displacement slightly, to obtain a good fit of the data.

As seen from Eq 2, the load relaxation of the spring is being modeled as creep deformation in the unstretched spring length. Creep is often modeled as the sum of an initial creep and a steady-state creep.[6,7] The following equations were used to simulate the primary and the steady-state creep, ε_i and ε_s, respectively, of the spring material (the creep of the fixture was nil):

$$\frac{d\varepsilon_i}{dt} = \left(\frac{F}{F_{ref}}\right)^M \exp\left(A - \frac{E}{RT}\right) \exp\left(\frac{-\varepsilon}{\delta}\right) \quad \text{(Eq 3a)}$$

$$\frac{d\varepsilon_s}{dt} = \left(\frac{F}{F_{ref}}\right)^M \exp\left(B - \frac{E}{RT}\right) \quad \text{(Eq 3b)}$$

where A and B are rate constants, δ is a scale for the initial creep, R is the universal gas constant, M is the force power, F_{ref} is a scale for the force, and E is the activation energy for creep. The total creep (ε) is the sum of the initial and steady-state creep.

Typically, the primary creep is modeled as exponentially decreasing with time.[7] However, these models all were developed for constant temperature tests. Since a model that can be applied to arbitrary temperature transients is required, it is expected that the initial creep will decay based on an integrated temperature history and not a simple function of time. Since the integrated creep (ε) is dependent upon an integrated temperature history, it is believed that this variable can be used to scale the decay of the initial creep. A comparison of our space-based model with the typical time-based model is presented in the Appendix.

It also should be noted that this model uses the same force power law and activation energy for both the primary creep and the steady-state creep. It is possible that these parameters may differ from one another, but to keep the number of parameters to a minimum, the same values are used for the initial and steady-state creep. The force exponent was set to 5, which is consistent with published data for deformation by dislocation climb.[8]

To complete the model, the spring constant is written as a function of temperature by using Eq 1. As noted above, the shear modulus is a function of temperature and was measured independently[4] by acoustic methods. As shown in Fig. 5, the acoustic results for drawn and aged Elgiloy shows a nearly linear decrease in the shear modulus with temperature. Thus, the following equation for the spring constant variation with temperature was used:

$$k = k_{ref}\,(1 - \eta[T - T_0]) \quad \text{(Eq 4)}$$

where k_{ref} was determined from ambient temperature measurements, and η is a constant chosen to simulate the reduction in the shear modulus with temperature.

By combining Eq 2, 3, and 4, a model describing the relaxation of the spring was constructed. The model has four free parameters (i.e., A, B, E, and δ) that can be determined by fitting to experimental data.

3.2 Model Calibration

A series of isothermal tests were performed to enable the calibration of the model (i.e., the determination of the free parameters). In these tests, springs from the same lot were extended to a displacement equal to their actual operational displacement of 1.2 mm. The corresponding force was approximately 450 mN at this displacement. The springs then were heated to a specified temperature and held there for a period of time while the load was monitored. At the end of the isothermal hold, the spring was allowed to cool, and the force was monitored during the cool-down period as well. Since, as noted above, a displacement of 1.2 mm resulted in time-independent plastic strains at 700 °C, only the constant temperature tests conducted at or below 650 °C were used to calibrate the model. Figure 7 shows the thermal cycles associated with the isother-

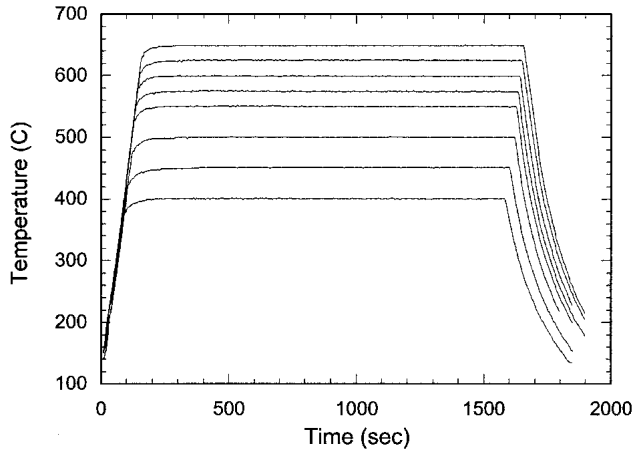

Fig. 7 Thermal cycles used for the model calibration tests

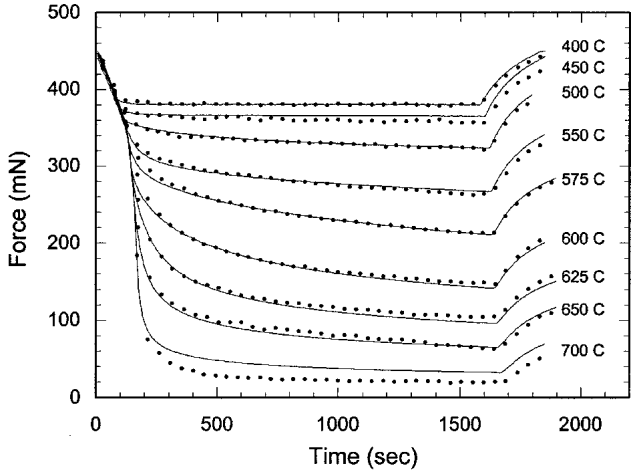

Fig. 8 Comparison of model prediction (solid lines) to data (points) for the isothermal calibration tests

mal calibration tests. It is important to note that, although the heating was conducted at as high a rate as possible that was consistent with good control and minimum overshoot (200 °C/min), the heat-up time is still appreciable. Moreover, some relaxation during the heating portion of the cycle could not be avoided, especially during the high-temperature tests. As a result, force data from the entire thermal cycle, including both the heat-up and cool-down time, were used in the determination of the free parameters.

Figure 8 shows a comparison of the experimental data with the fitted model. The excellent agreement results from choosing optimum values for the four free parameters. It is important to note that the entire data set of eight tests was fit simultaneously. The parameters do not vary from test to test. The 700 °C test is also included on this plot for comparison purposes. It was not used to determine the parameter values, and, since this spring experienced some time-independent plastic flow (yielding) at 700 °C, it is not surprising that the prediction for this test is not good.

Two of the fitting parameters are dimensional, so it is interesting to examine their values. The activation energy was determined to be 351 kJ/mol. This is higher than the cobalt self-diffusion activation energy, which is 268 kJ/mol.[9] However, Elgiloy contains a substantial amount of alloying elements, most notably Cr and Mo, which are known to increase creep strength. It is not uncommon for alloying to increase creep activation energies, so that the value of 351 kJ/mol is not considered unreasonable.

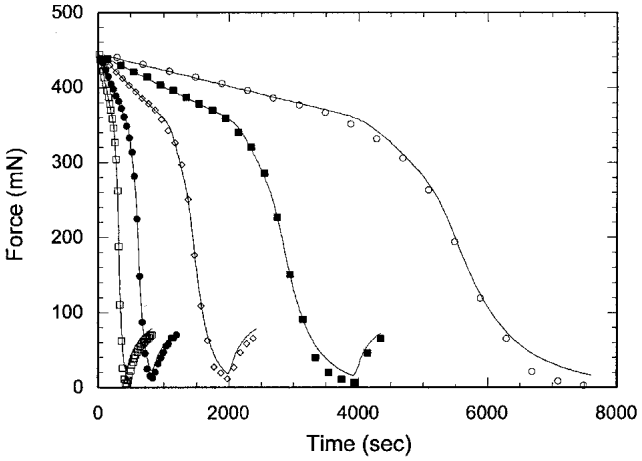

Fig. 9 Comparison of the model predictions and data from linear temperature ramp tests. The heating rates investigated were 5, 10, 20, 50, and 100 C/min.

The primary creep strain parameter (δ) value was determined to be 0.01. Thus, by the time the creep strain has reached 1%, the primary creep rate has been reduced by a factor of e (2.72). The primary creep dominates the creep of the spring material for the low-temperature tests. At temperatures above 550 °C, the steady-state creep becomes increasingly important in these tests. The 600 °C test resulted in 20% creep (as predicted by the model) based upon the initial spring length.

3.3 Model Validation

To validate the model, the experimental data of Fig. 6 were predicted by using the parameter constants determined from the model calibration. Figure 9 shows the results of these predictions, and the excellent agreement between the model and the data. These tests were linear ramps at 5, 10, 20, 50, and 100 °C/min from 150 °C to 800 °C, followed by a short cool-down period (these data are also presented in Fig. 6). To more fully validate the model and to verify its applicability to arbitrary thermal transients, a more complex stepwise heating cycle, which incorporated 100 °C/min ramps and 1 min isothermal holds at every 100 °C increments, was conducted. The thermal cycle associated with this test is shown in Fig. 10, and a comparison between the model prediction and the experimental results for this cycle is shown in Fig. 11. Clearly, the model accurately depicts the relaxation during this complex thermal cycle. Only results at temperatures above 700 °C show any significant disagreement between the experiments and the model, and this was expected due to the time-independent plastic deformation at this temperature.

It is stressed here that the validation tests are fundamentally

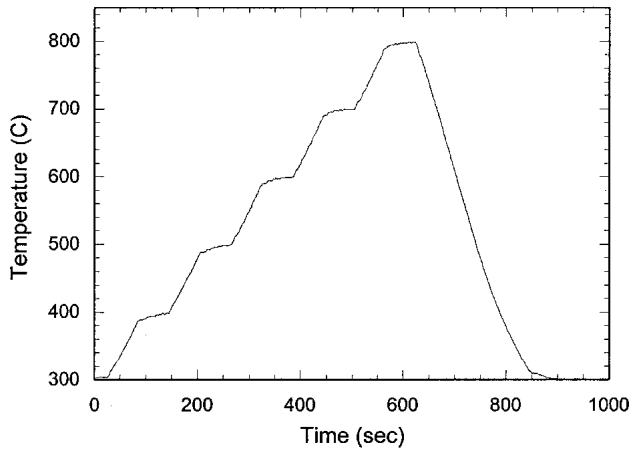

Fig. 10 Stepwise heating cycle used for further validation of the model

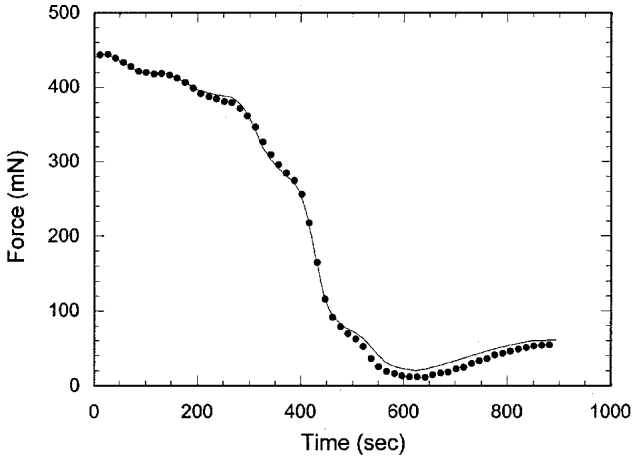

Fig. 11 Comparison of the model predictions to data for stepwise heating test

different in character than the calibration experiments. This helps to confirm the physical basis of the model used.

The transients depicted in Fig. 9 are of the most interest because these transients are very similar to what may occur during an abnormal thermal transient for many applications. Moreover, the slight inaccuracies at very high temperatures are not considered to be significant, since the springs have lost a major fraction of their force prior to reaching these temperatures.

3.4 Model Limitations and Extension

It is important to note that the model developed here applies only to helical extension springs fabricated from heat-treated Elgiloy. At this stage of the model development, it was intended to demonstrate the applicability of using creep kinetics (including both primary and steady state) as a basis for modeling the thermal stress relaxation of these types of springs under dynamic thermal conditions. However, we believe that the approach can be generalized to accommodate helical springs of other dimensions (made from Elgiloy).

The experimental program so far has focused primarily on transients with direct applications for a single spring. Clearly, a wider variety of experiments will further validate the model. Experimental tests in which the spring force is held constant and the displacement measured would help to further validate the model. Also, experiments with a variety of initial loads are needed, although the current model captures this effect to some extent because stress is constantly varying in the relaxation tests.

To extend the model to different springs of the same general type, an experimental program that examines a different number of coil turns and different coil and wire diameters is underway. In this way, the limitations can be more fully determined.

Currently, the creep of the spring is based upon the total spring length. Future models should probably consider basing this on the coil axial length, for the creep is probably better correlated with that parameter. The axial spring force is linearly related to the internal stress levels, so a model can be developed based on either parameter. However, if the model is to be extended to different spring geometries, it is probably easier to reformulate it in terms of the internal stress level instead of the axial spring force.

4. Conclusions

This report demonstrates a model for helical spring relaxation during abnormal thermal transients. The model incorporates both time-independent deformation mechanisms, such as thermal expansion and shear modulus changes, as well as time-dependent mechanisms, such as primary and steady-state creep. The model was shown to accurately predict the load relaxation behavior for continuous heating tests, as well as for a complex stepwise heating thermal cycle. To extend this model to other spring designs, further experimental data and model refinements may be required, but it appears that the approach described here is appropriate.

Acknowledgments

The authors would like to thank J.H. Gieske of Sandia National Laboratories for experimentally determining the elastic moduli for Elgiloy as a function of temperature. We would also like to thank D. Schmale for performing the spring force transient tests. This work was supported by the U.S. Department of Energy under contract DE-AC0494AL85000. Sandia is a multiprogram laboratory operated by Sandia Corporation, a Lockheed Martin Company, for the U.S. Department of Energy.

Appendix: Comparison of Models for Initial Creep

Models for transient constant temperature creep typically have the following form[7]:

$$\frac{d\varepsilon}{dt} = a\exp(-\gamma t) + b \qquad \text{(Eq A1)}$$

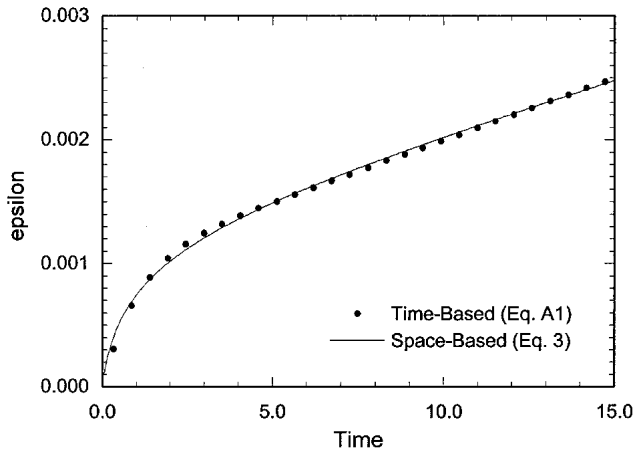

Fig. A1 Comparison of exponential time-based creep (symbols) fitted with exponential space-based creep.

where a is an initial creep rate that decays with time and b is a steady creep rate. By fitting to the experimental data, one can determine the free parameters a, b, and γ.

These parameters are typically a function of temperature, however, we will consider a constant temperature process here. A comparison is presented to show the equivalence between the traditional time-based model (Eq A1) and the space-based (displacement) model used in this article (Eq 3). The results generated from Eq A1 (using $a = 0.001$, $b = 0.0001$, and $\gamma = 1$) were fitted with the functional form of Eq 3. Figure A1 shows the comparison.

As can be seen from Fig. A1, reasonable fits can be obtained by using the space-based model presented in this article. This suggests that the space-based creep model may be just as viable as the time-based creep model. The space-based model may even be claimed to be superior since it can easily be extended to temperature transients, whereas the time-based model cannot.

One should note that if insufficient data are obtained after the initial creep has died away, it is impossible to use either model to obtain a good fit for the steady-state creep rate.

References

1. J.E. Shigley and C.R. Mische: *Mechanical Engineering Design*, McGraw-Hill Book Company New York, 1989, p. 413.
2. W.D. Hanna, D.J. Chang, and G.L. Steckel: "Stress Relaxation of Spring Materials" in *Proc. 32nd Aerospace Mechanisms Symposium*, S.W. Walker and Edward A Boesigner, ed., NASA/CP-1998-207191, National Aeronautics and Space Administration, John F. Kennedy Space Center, Cocoa Beach, FL, 13-15 May 1998, pp. 125-40.
3. S.V.V. Idermark and E.R. Johansson: "Room-Temperature Stress Relaxation of High-Strength Strip and Wire Spring Steels – Procedures and Data" in *Stress Relaxation Testing*, ASTM STP 676, Alfred Fox, ed., American Society for Testing and Materials, Philadelphia, PA, 1979.
4. J.H. Gieske: Sandia National Laboratories, Albuquerque, NM, 2002, personal communication.
5. J.H. Gieske: *Ultrasonic Measurement of Elastic Moduli of 17-4 PH Stainless Steel and Uranium – 2 Molybdenum from –40 Degrees C to 800 Degrees C*, Sandia National Laboratories Report SAND80-1121, Sandia National Laboratories, Albuquerque, NM, 1980.
6. L. Kloc, V. Skienicka, and J. Ventruba: "Comparison of Low Stress Creep Properties of Ferritic and Austenitic Creep Resistant Steels," *Mater. Sci. Eng.*, 2001, *A319-321*, pp. 774-78.
7. J.C.M. Li: "A Dislocation Mechanism of Transient Creep," *Acta Metall.*, 1963, *11*, pp. 1269-70.
8. R.W. Hertzberg: *Deformation and Fracture Mechanics of Engineering Materials*, 1st ed., John Wiley and Sons, New York, 1976, pp. 131-71.
9. Anonymous: *Smithells Metals Reference Book*, 6th ed., E.A. Brandes, ed., Butterworths, London, UK, 1983.